Environ. Sci. Technol. **2011,** *45,* 776–781

Evidence for Biomagnification of Gold Nanoparticles within a Terrestrial Food Chain

JONATHAN D. JUDY, JASON M. UNRINE, AND PAUL M. BERTSCH*

Department of Plant and Soil Sciences, University of Kentucky, Lexington, Kentucky 40546, United States

Received September 3, 2010. Revised manuscript received November 9, 2010. Accepted November 18, 2010.

Nanoparticles from the rapidly increasing number of consumer products that contain manufactured nanomaterials are being discharged into waste streams. Increasing evidence suggests that several classes of nanomaterials may accumulate in sludge derived from wastewater treatment and ultimately in soil following land application as biosolids. Little research has been conducted to evaluate the impact of nanoparticles on terrestrial ecosystems, despite the fact that land application of biosolids from wastewater treatment will be a major pathway for the introduction of manufactured nanomaterials to the environment. To begin addressing this knowledge gap, we used the model organisms *Nicotiana tabacum* L. cv *Xanthi* and *Manduca sexta* (tobacco hornworm) to investigate plant uptake and the potential for trophic transfer of 5, 10, and 15 nm diameter gold (Au) nanoparticles (NPs). Samples were analyzed using both bulk analysis by inductively coupled plasma mass spectrometry (ICP-MS) as well as spatially resolved methods such as laser ablation inductively coupled mass spectrometry (LA-ICP-MS) and X-ray fluorescence (μXRF). Our results demonstrate trophic transfer and biomagnification of gold nanoparticles from a primary producer to a primary consumer by mean factors of 6.2, 11.6, and 9.6 for the 5, 10, and 15 nm treatments, respectively. This result has important implications for risks associated with nanotechnology, including the potential for human exposure.

Introduction

Advances in nanotechnology have led to the development of many new consumer products containing nanomaterials and large increases in the mass and volume of several nanoparticles (NPs) produced. Silver (Ag) NPs have been studied extensively, due largely to their demonstrated antimicrobial effects (*1*). This property gives Ag NPs a wide variety of commercial applications, and their production and resultant environmental loading has increased to reflect this (*2, 3*). Titanium dioxide (TiO_2) and zinc oxide (ZnO) NPs are being used in products such as sunscreens, pharmaceuticals, and UV protective coatings (*4, 5*), and as these uses become more widespread, they will inevitably be discharged into the environment in increasing concentrations (*2*).

Between 2005 and 2010, the amount of listed products employing nanotechnology has increased from 54 to 1015 (*3*). As a result, the amount of nanomaterials entering waste streams is increasing steadily (*2*). During wastewater treatment, nanoparticles have been shown to concentrate in the sludge (*2*), 60% of which is applied to agricultural land as biosolids in the U.S. and the majority of Europe (*2*). Probabilistic material flow analysis models have predicted that between 2008 and 2012, the nanomaterials concentrations in sludge-treated soil in the U.S. will increase from 0.1 to 0.5 mg kg^{-1} for TiO_2 NPs, from 6.8 to 22.3 μg kg^{-1} for ZnO NPs, and from 2.3 to 7.4 μg kg^{-1} for Ag NPs (*2*).

Plant uptake (*6*), gastrointestinal absorption (*7*), and transmembrane transport of nanomaterials (*8*) have already been demonstrated. In the past, dietary exposure and trophic transfer have proven to be important terrestrial exposure pathways to chemicals such as polychlorinated biphenyls (PCBs), methylmercury, and dichlorodiphenyltrichloroethane (DDT) (*9*). Despite these facts, there has been little research published investigating the trophic transfer of nanoparticles and even less addressing the transfer from plants to animals. In one such study, trophic transfer was reported when freshwater algae (*Pseudokirchneriella subcapitata)* exposed to 10−25 nm CdSe quantum dots were fed to *Ceriadaphnia dubia* (*10*). Another study reported trophic transfer of 6 by 12 nm ellipsoid carboxylated and biotinated CdSe quantum dots from ciliated protozoans to rotifers (*11*). A recent publication presented evidence for the transfer of 21 nm TiO_2 NPs from *Daphnia magna* to *Danio rerio* (zebrafish) (*12*). We have demonstrated the accumulation of Au NPs up to 55 nm in diameter (*9*) and copper (Cu) NPs up to 100 nm in diameter in earthworms from exposure to NP spiked soil (*9, 13*). There are also some studies that provide indirect evidence of trophic transfer. In one such study, researchers presented indirect evidence that gold (Au) NPs transferred from the water column to the marine food web within estuarine mesocosms (*14*). Another study exposed *Caenorhabditis elegans* to ZnO, Al_2O_3, and TiO_2 NPs in the presence of *Escherichia coli* (*E. coli*), which were provided as food (*15*). It is possible that some of the NPs were internalized by the *E. coli* and transferred to the nematodes through dietary uptake.

These initial results suggest that NPs could be available for dietary uptake at lower trophic levels and subsequently transferred through terrestrial food webs. As terrestrial ecosystems are a possible pathway for human exposure (*16*), there is an urgent need to examine the transport and fate of NPs in terrestrial ecosystems under environmentally relevant scenarios. To begin addressing this knowledge gap, we used the model organisms *Nicotiana tabacum* L. cv *Xanthi* and *Manduca sexta* (tobacco hornworm) to investigate plant uptake and the potential for trophic transfer of 5, 10, and 15 nm diameter Au NPs. Au NPs are being used in a variety of applications including the detection and imaging of cancer cells (*17*), pharmaceuticals designed to combat HIV (*18*), and catalysis in fuel cells (*19*). We selected Au for this initial study due to its resistance to oxidative dissolution and release of dissolved Au ions as well as because of its low natural background concentrations (*20*). These properties make Au an ideal model to probe particle specific uptake in complex systems.

Based on previously published results (*6, 7, 9, 10, 12, 13*), we hypothesized that 5−15 nm Au NPs may be transferred through dietary exposure from a primary producer to a primary consumer. We also hypothesize that due to the presence of size selective physiological barriers, such as the plant cell wall, size will be an important factor in plant uptake and potential trophic transfer of Au nanoparticles. Finally,

* Corresponding author phone: (859)257-1651; e-mail: pmbert2@email.uky.edu. Corresponding author address: University of Kentucky, Department of Plant and Soil Sciences, N-212M, Agricultural Science Center North, Lexington, KY 40546.

10.1021/es103031a
Published on Web 12/03/2010

we hypothesize that Au nanomaterials will accumulate in the primary consumer from ingestion of the primary producer, or bioaccumulate, but that the Au NPs will not occur in a higher concentration in the primary consumer than seen in the tobacco, or biomagnify. This hypothesis is based on evidence demonstrating that metals ions, other than lipophilic complexes such as methyl mercury, do not typically biomagnify (*23*).

Experimental Section

Nanoparticle Characterization. Stable aqueous suspensions of 5, 10, and 15 nm diameter primary particle size gold (Au) nanoparticles surface modified with tannic acid and carrying a negative surface charge were purchased (Nanocomposix San Diego, CA USA) and characterized using transmission electron microscopy (TEM) and dynamic light scattering (DLS, see the Supporting Information, Table S1, Figure S3). Tannic acid coated nanoparticles were selected due to the fact that a suspension of bare gold nanoparticles would be unstable under these exposure conditions and would aggregate, making it very difficult to investigate differences in uptake based on size. Additionally, tannic acid is one of only a few environmentally relevant coatings available in our desired size range and surface charge with low polydispersivity. We also consider a tannic acid coated NP to be a reasonable analog for a particle coated with natural organic matter, which we believe will adsorb to nanoparticle surfaces once introduced into soil, similar to soil minerals (*24*).

The stock suspension was diluted to create the treatment suspensions. Mean hydrodynamic diameters and electrophoretic mobilities of the nanoparticle treatment suspensions were measured using a Nano-ZS zetasizer and were conducted at a suspension concentration of 100 mg Au L^{-1} (Malvern, Worcestershire, UK). The 100 mg L^{-1} concentrations were verified through ICP-MS measurement and averaged 100.9 ± 4.61 mg L^{-1}. TEM size analysis was provided by the manufacturer (Nanocomposix San Diego, CA USA). The manufacturer fixed the particles on Formvar/carbon-coated copper transmission electron microscope (TEM) grids 200 mesh size (Ted Pella, Redding, CA). Imaging was performed on a Jeol 1010 TEM, and the diameters of 103 randomly selected individual particles were quantified with Image J software (see Supporting Information, Figure S1). Particle size distribution for each size class is based on the relative percent of the total particle diameters measured (see Supporting Information, Figure S2).

Exposure of the Primary Producer. *Nicotiana tabacum* L. cv *Xanthi* was selected as a model primary producer for this study due to its ability to bioconcentrate heavy metals (*25*) as well as its similarity to *Lycopersicon esculentum* (tomato), a USEPA recommended test plant for uptake and translocation (*26*) and a member of the Solanacae family of plants (*27*). *Nicotiana tabacum* L. cv *Xanthi* seeds were sterilized by shaking with 6% sodium hypochlorite for 10 min and washing three times with 18 MΩ deionized water (DI) (*26*). Seeds were then placed in plates of gellan gum (Phytagel, Sigma-Aldritch, St. Louis, MO USA) containing a half strength nutrient mixture (Phytotechnology Laboratories, Shawnee Mission, KS USA) and grown in a greenhouse at a mean temperature of 25.4 ± 1.7 °C, with a mean relative humidity of 81.6 ± 9.8% and a 12 h light cycle. After four weeks, the plants were randomly divided into treatment populations, placed in microcentrifuge tubes, and grown for one week in either 1.5 mL of DI or 5, 10, or 15 nm nanoparticles suspended in DI at 100 mg Au L^{-1}. Treatments were periodically adjusted to the initial volume with DI.

Exposure of the Primary Consumer. We selected *Manduca sexta* as a model consumer for this study due to its ability to digest tobacco, which is a result of its unique gut chemistry (*28, 29*). *Manduca sexta* larvae generate a pH gradient in their gut that ranges between 5 and 12 (*28*) and an Eh gradient that that varies between −188 to 172 mV (*29*), either of which could play a role in the dietary uptake of NPs. This high pH is thought to be an adaptation to tannin-rich diets and is most likely the result of ion transport (*28, 29*). *Manduca sexta* eggs were purchased from Great Lakes Hornworm (Grand Rapids, MI, USA). The hornworms were randomly divided into their individual treatment enclosures at the beginning of the second larval instar, during which the hornworms were 9−18 mm long (*30, 31*). Five hornworms were provided living plants growing in DI, and 10 hornworms each were provided living plants growing in DI that were previously exposed to the 5, 10, and 15 nm Au treatment suspensions as described above. The hornworm enclosures consisted of a 48.1 mL vial containing a 3 mL vial filled with DI, which was placed inside and glued to the bottom (see Supporting Information, Figure S3). A 2−3 mm diameter hole was punched into the inner vial cap through which tobacco roots were threaded, with the leaves of the living plant resting on the top of the inner vial cap. This exposure setting was designed to disallow the hornworms access to the plant roots. Plants were rinsed with DI using a wash bottle and then submerged in water twice before transfer to the hornworm enclosures. The hornworms were then added to the enclosures, which were covered with nylon mesh. Enclosures were cleaned daily to reduce the incidence of disease.

When the hornworms had consumed the majority of the leaf material of their initial plants, a new plant was placed into their enclosure. The feeding cycle continued for one week. Each plant was weighed before and after placing it in the enclosures, and the final mass of tobacco consumed by each hornworm was recorded. To maximize the mass of tobacco tissue available to feed to each hornworm, tobacco tissue samples for the tobacco bulk analysis consisted of small triangles of tissue cut using a razor blade from a leaf tip of each individual plant that was fed to each hornworm. For each hornworm, leaf tip samples from each plant that was fed to the hornworm were pooled for bulk analysis.

Entire hornworms were embedded in hydrophilic glycol methacrylate resin and sectioned to approximately 1 mm using a diamond wafering blade. Several hornworm sections were cut perpendicularly to the body axis for each sample and were each keyed to standard anatomical divisions of the *Manduca sexta* larvae (*30*). Hornworm sections from the midgut (*30*) and whole tobacco leaves were mounted on metal free polyimide film (Kapton; Dupont, Wilmington, DE). Hornworm sections were analyzed using X-ray absorption near edge spectroscopy (μXANES) and synchrotron X-ray fluorescence microprobe (μXRF) scans. Whole tobacco leaves were analyzed using μXRF and laser ablation inductively coupled mass spectrometry (LA-ICP-MS). Hornworm cross sections from an earlier identical experiment with a smaller overall n were also mapped using μXRF.

Laser Ablation Inductively Coupled Mass Spectrometry (LA-ICP-MS). LA-ICP-MS depth profiles were collected using sequential controlled laser bursts from a LSX-213 laser ablation system (Cetac, Omaha, NE, USA) that removed 400 × 400 μm^2 craters, the depth of which ranged from 8−10 μm as measured using a Nikon Eclipse 90i light microscope (Nikon, Tokyo, Japan). The material removed during each laser pulse was measured using an Elan DRC Plus ICP-MS (PerkinElmer-Sciex, Waltham, MA). Six depth profiles from 3 samples were collected for each treatment. For each sample, one depth profile was collected from the leaf mesophyll, and one was collected from the leaf midrib.

Synchotron X-ray Analysis. μXRF measurements of gold were based on the fluorescence from the L-α edge (9,713 eV (*32*)) and were conducted at beamline X-26A at the National Synchrotron Light Source at Brookhaven National Laboratory (Upton, NY, USA) using a nine element Ge array detector

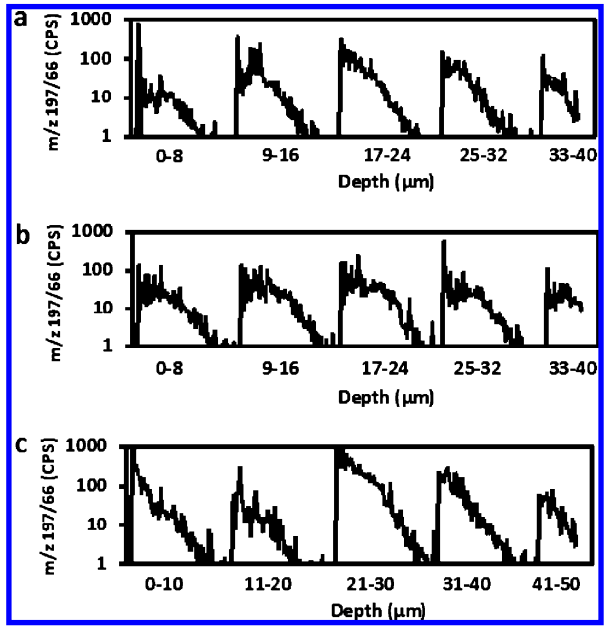

FIGURE 1. Laser ablation inductively coupled mass spectrometry (LA-ICP-MS) depth profiles from mesophyll of tobacco leaves exposed to a, **5 nm,** b, **10 nm, and** c, **15 nm gold nanoparticles. The presence of gold within leaf tissue removed during each laser burst demonstrates the presence of gold throughout the leaf. Gold concentration reported as log counts per second (CPS) of *m/z* 197 (Au) normalized by CPS for *m/z* 66 (Zn) to account for the mass of tissue removed from each laser burst.**

(Canberra, Meridian, CT). The X-ray beam was monochromatized at 13 keV. The beam had a spot size of 9 μm horizontally and 5 μm vertically. The beam was translated through the sample in 20 μm steps, and spectra were collected at each step for one second. Au L absorption edge (11,921 eV) μXANES was performed in fluorescence mode by scanning the monochromator from 11850 to 12038 eV with 2 eV steps. μXANES spectra were analyzed using the Athena software package (*33*). The beam was calibrated to the absorption edge using a Au foil standard. μXANES spectra from the Au foil standard as well as from a gold chloride standard were collected for comparison to μXANES spectra in the samples.

Inductively Coupled Plasma-Mass Spectrometry Analysis of Bulk Tissue. Wet tobacco samples were weighed and placed in microcentrifuge tubes. The samples were digested in 50 μL of hydrogen peroxide and 150 μL of nitric acid. The tubes were heated overnight at 60 °C in an Isotemp 2001 FS hot block (Fisher Scientific, Pittsburgh, PA). In the morning, 300 μL of hydrochloric acid was added, and the samples were heated in the hot block for an additional 4 h, after which the digestate was collected and brought to 3 mL volume. Each digestate was analyzed by ICP-MS using an Elan DRC Plus ICP-MS (PerkinElmer-Sciex, Waltham, MA). Moisture content of the tobacco leaves was measured to average 91.1% ± 1.9%, and the results of the tobacco bulk analysis were adjusted to dry weight using this estimate. Surviving hornworms were dried for 48 h at 60 °C and subsequently digested using the same protocol. Analytical runs contained calibration verification samples, duplicate dilutions, and spike recovery samples. As there is no widely available standard reference material containing gold, a standard reference material was synthesized using finely ground dried tobacco leaves spiked with gold standard to a concentration of 10 mg kg^{-1}. Mean standard recovery using this material was 103.6%. Spike recovery averaged 94.2%, and the mean relative percent difference between duplicate dilutions was 7.4%.

Results and Discussion

Concentrations of Au in whole, undried tobacco leaves were below the detection limits as determined by synchrotron μXRF. However, ICP-MS analysis of dried tobacco tissue revealed mean gold concentrations of 40.3, 95.8, and 61.7 mg Au kg^{-1} dry tobacco in the 5, 10, and 15 nm treatments, respectively. All of the LA-ICP-MS depth profiles of tobacco leaves that were collected provided similar results and verified that gold was present throughout the plant tissue cross section, rather than just on the leaf surface (Figure 1). These results differ from the results from one early study where barley (*Hordeium vulgare* L.) was exposed to bare 4.6 nm diameter and 5.8 nm polyvinylpyrolidone (PVP) coated Au NPs for were used as opaque electron tracers with no uptake or translocation observed using electron microscopy over exposure periods of 41 or 22 h, respectively (*34*). The differences in the exposure durations or detection methodology between this early study and the work presented here could be responsible for the differences in the results

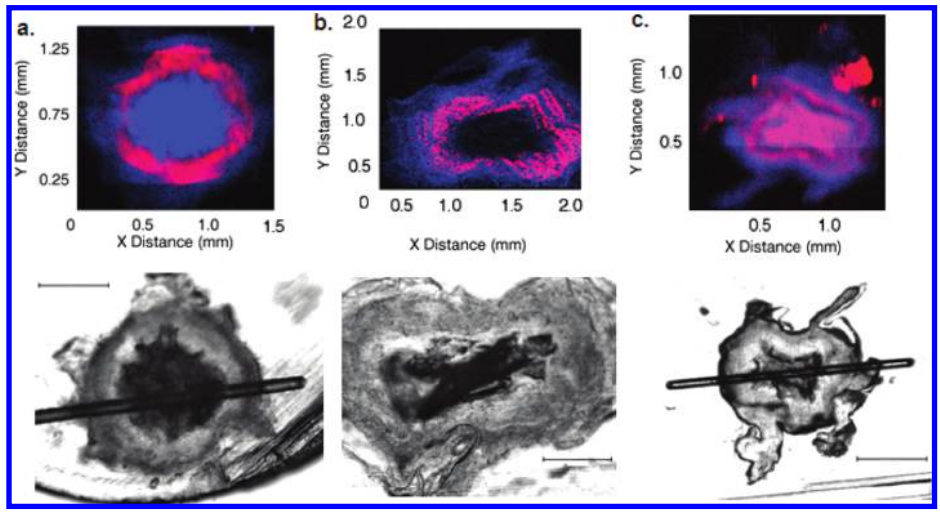

FIGURE 2. Synchrotron X-ray fluorescence microprobe (μXRF) maps of fluorescence from the Au L-α edge of gold (Au), depicted in red, and zinc (Zn), depicted in blue, as well as light micrographs of cross sections of *Manduca sexta* specimens that were fed plants exposed to a, **5 nm nanoparticles** b, **10 nm nanoparticles and** c, **15 nm nanoparticles. Au fluorescence, reported in counts per second (CPS), was detected throughout the hornworm tissues surrounding the gut lumen. *Manduca sexta* sections are from the midgut of each hornworm (*30*). Scale bars in the light micrographs are each equal to 0.5 mm. Lines crosscutting the light micrographs for sections a. and c. are from collecting LA-ICP-MS transects across these sections.**

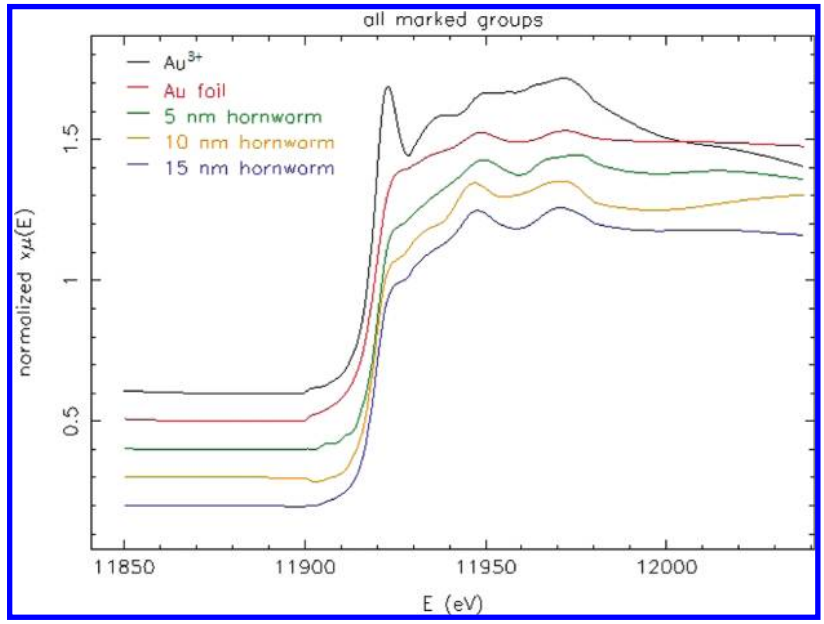

FIGURE 3. X-ray absorption near edge spectroscopy (XANES) spectra for gold foil, Au^{3+} as gold chloride ($HAuCl_4$), gold hotspots within cross sections of hornworm fed tobacco treated with each of the three nanoparticle sizes (5, 10, and 15 nm hornworm), and samples of the original dosing material (5, 10, and 15 nm Au). The absence of the peak diagnostic of $HAuCl_4$ in the XANES spectra indicates that only Au^0 was present within hornworm tissues and that there were no Au ions in the dosing material.

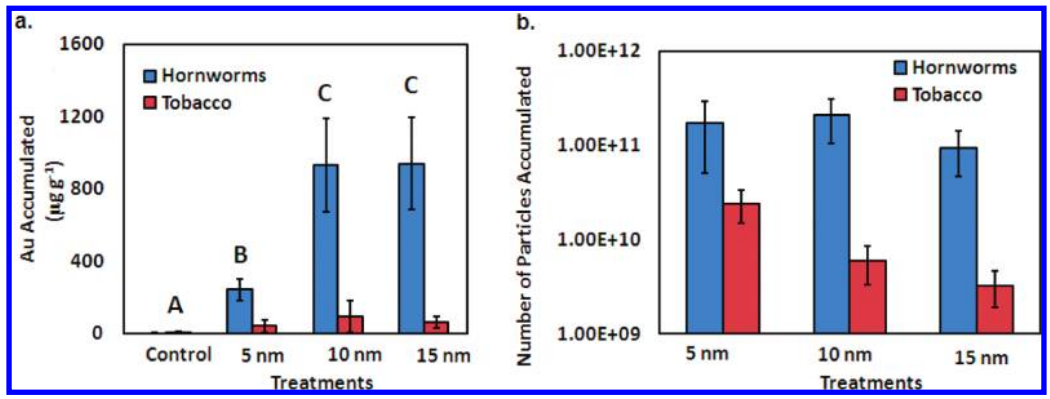

FIGURE 4. Bulk gold (Au) concentration reported as mean ± one standard error for tobacco and hornworms based on a.) mass and b.) particle number. Groups with the same letter are not significantly different from each other.

reported. It is also possible that the tannic acid coating stabilizes gold particles in a natural system more than PVP. However, how surface coating affects plant uptake and trophic transfer is currently unclear. Regardless, plant uptake of 15 nm diameter NPs is consistent with recently published research on plant uptake of nanoparticles, which has reported uptake of 30−50 nm copper particles (*35*) and 20 nm iron oxide particles (*36*).

Manduca sexta from each of the populations exposed to NPs accumulated Au in the tissue surrounding the gut lumen in concentrations detectable by synchrotron μXRF (Figure 2). Although Au is not expected to be oxidized under the conditions of this experiment, we validated this by collection of μXANES at Au hotspots elucidated by the μXRF scans of hornworm cross sections from each treatment. These spectra were compared to Au foil and gold chloride ($HAuCl_4$) standards, which clearly indicate that only Au^0 was present within hornworm tissues (Figure 3). Additionally, samples of the treatment suspensions were filtered through a 3 kDa membrane and analyzed for Au using ICP-MS, which confirmed that the amount of dissolved gold in the dosing material was negligible, providing additional evidence that the Au transferred to the hornworm via plant consumption was via Au NPs rather than as dissolved gold ions (see the Supporting Information, Table S1).

The mass of Au transferred was quantified by comparing the bulk analyses of the tobacco and hornworm tissues, which demonstrated that Au concentrations in the hornworm tissue exceeded that of the tobacco tissue by mean factors of 6.2, 11.6, and 9.6 for the 5, 10, and 15 nm treatments, respectively (Figure 4a). The bulk analysis data were log transformed and analyzed using ANOVA and posthoc multiple pairwise comparisons of the means of the Au concentration in the hornworms for each treatment at $\alpha = 0.05$ using the Student−Newman−Keuls procedure. The SNK procedure grouped the control population alone, the 5 nm population alone, and the 10 and 15 nm populations together (see Supporting Information, Table S2). Assumptions of normality and homoscedasticity were tested using Shapiro-Wilk's test and Barlett's test. The mass of Au transferred was also converted to number of particles transferred (Figure 4b), which indicated that there was no significant difference between the number of particles transferred between treatments.

The concentration of Au measured in the hornworm tissues, though consistent with our first hypothesis, was unexpectedly high and implies that under certain conditions, stable NPs as large as 15 nm may be available for transfer to higher trophic levels with the potential for biomagnification, contrary to our third hypothesis. The bulk concentration data

also demonstrate that the mass of Au in the hornworm tissues for the 10 and 15 nm treatments was significantly higher than the 5 nm treatment (Figure 4), inconsistent with our second hypothesis. The observed trend is similar to that demonstrated in previous work on the uptake of 10−100 nm Au NPs into mammalian cells (*8*) and could be due to smaller particles being more tightly bound to membrane receptors (*8*). This trend could also be due to differences in zeta potential and pH between the treatment solutions rather than the size of the NPs, as the 10 and 15 nm treatment suspensions had virtually identical zeta potentials (see Supporting Information, Table S1). Additionally, the 10 and 15 nm NPs had similar hydrodynamic diameters (see Supporting Information, Table S1). The similarity in uptake between these two treatments may reflect the greater importance of hydrodynamic diameter over primary particle size in NP uptake. The differences in uptake between the treatments could also be an effect of particle number, as the concentrations of Au in the hornworms based on particle number were not significantly different between treatments (Figure 4b). However, it is problematic to analyze trends based on particle number, as the dosages by particle number would be different for each treatment.

Of the previous studies that have been conducted investigating the trophic transfer of nanomaterials, none have considered terrestrial environments, and many have neglected to conduct crucial analyses. For example, spatial analysis of exposed organisms is required to verify that NP uptake and transfer has occurred, as opposed to the NPs being adsorbed to the external surfaces of the organisms, a very common occurrence with aquatic plants. Additionally, in many cases metal ions can be solubilized from NPs during the course of an experiment (*37*), and bulk analysis cannot discriminate metals in NP or ionic forms nor whether the nanomaterials are adsorbed to the surface of an organism or have been incorporated into the organism's tissues.

This study presents the first evidence of trophic transfer of NPs from a terrestrial primary producer to a primary consumer as well as the first evidence of biomagnification of NPs within a terrestrial food web. Past experience with chemicals such as methylmercury, DDT, and PCBs have revealed dietary uptake at lower trophic levels and accumulation up the food chain to be an important route of contaminant exposure, resulting in chronic or even acute toxicity to a variety of ecoreceptors as well as humans (*9*). Our observation that NPs can biomagnify highlights the importance of considering dietary uptake as a pathway for NP exposure and raises questions about potential ecoreceptor and human exposure to NPs from long-term land application of biosolids containing NPs.

Acknowledgments

The authors acknowledge the advice and assistance of W. Shoults-Wilson, W. Rao, A. Lanzirotti, R. Lewis, and L. Newman. Major funding for this research was provided by the National Science Foundation (NSF) and the Environmental Protection Agency (EPA) under NSF Cooperative Agreement EF-0830093, Center for the Environmental Implications of NanoTechnology (CEINT). J. Unrine was supported by U.S. EPA through Science to Achieve Results Grant (RD 833335). This research was also partially supported by a grant from the U.S. Environmental Protection Agency's Science to Achieve Results (STAR) program (RD834574). Any opinions, findings, conclusions, or recommendations expressed in this material are those of the author(s) and do not necessarily reflect the views of the NSF or the EPA. This work has not been subjected to NSF or EPA review, and no official endorsement should be inferred. Portions of this work were performed at Beamline X26A, National Synchrotron Light Source (NSLS), Brookhaven National Laboratory. X26A is supported by the Department of Energy (DOE) - Geosciences (DE-FG02-92ER14244 to The University of Chicago - CARS) and DOE - Office of Biological and Environmental Research, Environmental Remediation Sciences Div. (DE-FC09-96-SR18546 to the University of Kentucky). Use of the NSLS was supported by DOE under Contract No. DE-AC02-98CH10886.

Supporting Information Available

TEM micrographs of nanoparticle suspensions, data from the characterization of the nanoparticles used in this study including particle size distributions, a picture of the exposure setting, and details from the Student−Newman−Keuls comparison on the mean gold concentrations in the hornworms. This material is available free of charge via the Internet at http://pubs.acs.org.

Literature Cited

(1) Sondi, I.; Salopek-Sondi, B. Silver nanoparticles as antimicrobial agent: a case study on *E. coli* as a model for Gram-negative bacteria. *J. Colloid Interface Sci.* **2004**, *274*, 177–182.

(2) Gottshalk, F.; Sonderer, T.; Scholz, R. W.; Nowack, B. Modeled Environmental Concentrations of Engineered Nanomaterials (TiO_2, ZnO, Ag, CNT, Fullerenes) for Different Regions. *Environ. Sci. Technol.* **2009**, *43* (24), 9216–9222.

(3) Woodrow Wilson International Center for Scholars. The Project on Emerging Nanotechnologies. 2010. Available at http://www.nanotechproject.org/inventories/consumer/analysis_draft/ (accessed August 1, 2010).

(4) Aitken, R. J.; Chaudhry, M. Q.; Boxall, A. B. A.; Hull, M. Manufacture and use of nanomaterials: current status in the UK and global trends. *Occup. Med.* **2006**, *56*, 300–306.

(5) Cross, S. E.; Innes, B.; Roberts, M. S.; Tzuzuki, T.; Robertson, T. A.; McCormick, P. Human Skin Penetration of Sunscreen Nanoparticles: In-vitro Assessment of a Novel Micronized Zinc Oxide Formulation. *Skin Pharmacol. Physiol.* **2007**, *20*, 148–154.

(6) Lin, S.; Reppert, J.; Hu, Q.; Hudson, J. S.; Reid, M. L.; Ratnikova, T. A.; Rao, A. M.; Luo, H.; Ke, P. C. Uptake, Translocation, and Transmission of Carbon Nanomaterials in Rice Plants. *Small* **2009**, *5* (10), 1128–1132.

(7) Hillyer, J. F.; Albrecht, R. M. Gastrointestinal persorption and tissue distribution of differently sized colloidal gold nanoparticles. *J. Pharm. Sci.* **2002**, *90*, 1927–1936.

(8) Chithrani, B.; Ghazani, A. A.; Chan, W. C. W. Determining the size and shape dependence of gold nanoparticle uptake into mammalian cells. *Nano Lett.* **2006**, *6* (4), 662–668.

(9) Unrine, J. M.; Bertsch, P. M.; Hunyadi, S. E. In *Nanoscience and Nanotechnology: Environmental and Health Impacts*; Grassian, V. H., Ed.; John Wiley and Sons, Inc.: Hoboken, 2008.

(10) Bouldin, J.; Ingle, T.; Sengupta, A.; Alexander, R.; Hannigan, R.; Buchanan, R. Aqueous toxicity and food chain transfer of quantum dots in freshwater algae and *Ceriodaphnia dubia*. *Environ. Toxicol. Chem.* **2008**, *27* (9), .

(11) Holbrook, R. D.; Murphy, K. E.; Morrow, J. B.; Cole, K. D. Trophic transfer of nanoparticles within a simplified invertebrate food web. *Nat. Nanotechnol.* **2008**, *3*, 352–355.

(12) Zhu, X.; Wang, J.; Zhang, X.; Chang, Y.; Chen, Y. Trophic transfer of TiO_2 nanoparticles from daphnia to zebrafish in a simplified freshwater food chain. *Chemosphere* **2010**, *79* (9), 928–933.

(13) Unrine, J. M.; Tsyusko, O. V.; Hunyadi, S. E.; Judy, J. D.; Bertsch, P. M. Effects of Particle Size on Chemical Speciation and Bioavailability of Copper to Earthworms (*Eisenia fetida*) Exposed to Copper Nanoparticles. *J. Environ. Qual.* 2010, doi:10.2134/jeq2009.0387.

(14) Ferry, J.; Craig, P.; Hexel, C.; Sisco, P.; Frey, R.; Pennington, P. L.; Fulton, M. H.; Scott, I. G.; Decho, A. W.; Kashiwada, S.; Murphy, C. J.; Shaw, T. J. Transfer of gold nanoparticles from the water column to the estuarine food web. *Nat. Nanotechnol.* **2009**, *4*, 441–444.

(15) Wanga, H.; Wicka, R.; Xing, B. Toxicity of nanoparticulate and bulk ZnO, Al_2O_3 and TiO_2 to the nematode Caenorhabditis elegans. *Environ. Pollut.* **2008**, *154* (4), 1171–1177.

(16) U. S. Environmental Protection Agency. *A Guide to the Biosolids Risk Assessements for the EPA Part 503 Rule*; EPA: Washington, DC, 1995.

(17) El-Sayed, I.; Huang, X.; El-Sayed, M. A. Surface Plasmon Resonance Scattering and Absorption of anti-EGFR Antibody Conjugated Gold Nanoparticles in Cancer Diagnostics: Applications in Oral Cancer. *Nano Lett.* **2005**, *5* (5), 829–834.

(18) Bowman, M.; Ballard, T. E.; Ackerson, C. J.; Feldhein, D. L.; Margolis, D. M.; Melander, C. Inhibition of HIV Fusion with Multivalent Gold Nanoparticles. *J. Am. Chem. Soc.* **2008**, *130*, 6896–6897.
(19) Kim, B. W.; Voitl, T.; Rodriguez-Rivera, J. G.; Dumesic, J. A. Powering Fuel Cells with CO via Aqueous Polyoxometalates and Gold Catalysts. *Science* **2004**, *305* (5688), 1280–1283.
(20) Merchant, B. Gold, the noble metal and the paradoxes of its toxicology. *Biologicals* **1998**, *26* (1), 49–59.
(21) Smith, J. A.; Witkowski, P. J.; Fusillo, T. V. *Manmade organic compounds in the surface waters of the United States—A review of current understanding*; 92 U. S. Geological Survey: Reston, 1988.
(22) Nowell, L. H.; Capel, P. D.; Dileanis, P. D., 1999,. *Pesticides in stream sediment and aquatic biota—distribution, trends, and governing factors*, 1001 Lewis Publishers: Boca Raton, FL, 1999.
(23) Wren, C. D.; Macrimmon, H. R.; Loescher, B. R. Examination of bioaccumulation and biomagnification of metals in a precambrian shield lake. *Water, Air, Soil Pollut.* **1982**, *19* (3), 277–291.
(24) Gu, B.; Schmitt, J.; Chen, Z.; Llang, L.; McCarthy, J. Adsorption and Desorption of Natural Organic Matter on Iron Oxide: Mechanisms and Models. *Environ. Sci. Technol.* **1994**, *28*, 38–46.
(25) Raskin, I.; Nanda Kumar, P. B. A.; Dushenkov, S.; Salt, D. E. Bioconcentration of heavy metals by plants. *Curr. Opin. Biotechnol.* **2004**, *5*, 285–290.
(26) U. S. Environmental Protection Agency. *Ecological Effects Test Guidelines: OPPTS 850.4800 Plant Uptake and Translocation Test*; EPA: Washington, DC., 1996.
(27) U. S. Department of Agriculture. *Germplasm Resources Information Network (GRIN)*; National Germplasm Resources Laboratory: Beltsville, MD, 2010.
(28) Dow, J. pH Gradients in Lepidopteran Midgut. *J. Exp. Biol.* **1992**, *172* (1), 355–375.
(29) Appel, H. Gut Redox Condition in Herbivorous Lepidopteran Larvae. *J. Chem. Ecol.* **1990**, *16* (12), 3277–3290.
(30) Eaton, J. *Lepidopteran Anatomy*; Wiley Interscience: New York, 1988.
(31) Reineke, J. P.; Buckner, J. S.; Grugel, S. R. Life Cycle of Laboratory-Reared Tobacco Hornworms, *Manduca sexta*, A study of development and Behavior, Using Time-Lapse Cinematography. *Biol. Bull.* **1980**, *158*, 129–140.
(32) Thompson, A.; Attwood, D.; Gullikson, E.; Howells, M.; Kim, K.; Kirz, J.; Kortright, J.; Lindau, I.; Pianetta, P.; Robinson, A.; Scofield, J.; Underwood, J.; Vaughan, D.; Williams, G.; Winick, H. *Center for X-Ray Optics and Advanced Light Source X-Ray Data Booklet*; Lawrence Berkley National Laboratory: Berkeley, 2009.
(33) Ravel, B.; Newville, M. Athena, Artemis, Hephaestus: Data analysis for X-ray absorption spectroscopy using IFEFFIT. *J. Synchrotron Radiat.* **2005**, *12*, 537–541.
(34) Robards, A. The entry of ions and molecules into roots: an investigation using electron-opaque tracers. *Planta* **1974**, *120*, 1–12.
(35) Lee, W.; An, Y. J.; Yoon, H.; Kweon, H. S. Toxicity and bioavailability of copper nanoparticles to the terrestrial plants mung bean (*Phaseolus radiatus*) and wheat (*Triticum aestivum*): plant agar test for water-insoluble nanoparticles. *Environ. Toxicol. Chem.* **2007**, *27* (9), 1915–1921.
(36) Zhu, H.; Han, J.; Xiao, J.; Jin, Y. Uptake, translocation, and accumulation of manufactured iron oxide nanoparticles by pumpkin plants. *J. Environ. Monit.* **2008**, *10*, 713–717.
(37) Derfus, A. Probing the Cytotoxicity of Semiconductor Quantum Dots. *Nano Lett.* **2003**, *4* (1), 11–18.

ES103031A